Laser Writing of Metallic Nanostructures in a Polymer Matrix with Applications to Metamaterials

Shobha Shukla[1], Xavier Vidal[2], Edward P. Furlani[2,3,4], Mark T. Swihart[2,4], Paras N. Prasad[2,3,5]

School of Engineering and Applied Sciences[1], Harvard University, Boston, MA
Institute of Lasers, Photonics and Biophotonics[2], Departments of Electrical Engineering[3], Chemical and Biological Engineering[4], and Chemistry[5],
University at Buffalo (SUNY), NY

ABSTRACT

We present a novel laser-based method for fabricating metallic nanostructures in a polymer matrix with sub-wavelength resolution. The method involves two-photon lithography (TPL) in which a femtosecond-pulsed laser induces two-photon initiated *in situ* reduction of a metal salt and simultaneous polymerization of a negative photoresist. We discuss details of the laser writing process and demonstrate various fabricated functional structures along with simulations of their electromagnetic behavior.

Keywords: two photon lithography, laser writing of subwavelength metallic structures, nanofabrication, plasmonic nanostructures, polymer metamaterials.

1 INTRODUCTION

Interest in two-photon lithography (TPL) has grown dramatically in recent years, especially for applications that require fabrication of three-dimensional microstructures with subwavelength resolution [1, 2] Conventional lithographic techniques are not well suited for this as they are inherently limited to two-dimensional processing [1, 3-4]. However, three-dimensional TPL using photopolymers overcomes these limitations and has found broad application in fields such as micro/nanofluidics, biotechnology and photonics. To date, most TPL applications have involved the fabrication of non-metallic structures, and only recently has progress been reported on TPL-based fabrication of metallic micro and nanostructures [5]. The ability to write three-dimensional metallic structures in a polymeric matrix is of great interest as it holds potential for disruptive advances in emerging fields such as photonics, flexible electronics, metamaterials and plasmonics.

In this presentation we demonstrate a novel method for producing metallic nanostructures with sub-wavelength resolution in a polymer matrix. These structures are written within a photoresist film using a femtosecond-pulsed laser to induce two-photon initiated *in situ* reduction of a metal salt and simultaneous polymerization of a negative photoresist (Figs. 1-2). Structures with linewidths from 150 nm to over 1000 nm have been prepared and characterized.

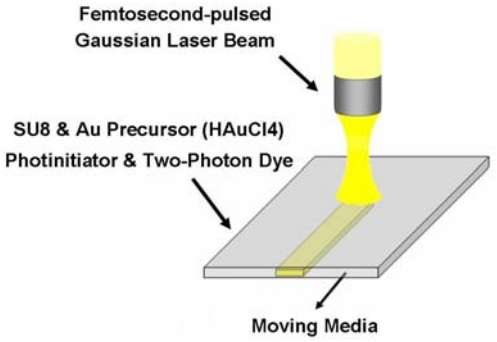

Figure 1: Illustration of TPL writing process.

The individual *in situ*-generated metallic nanoparticles are a few nanometers in diameter and metallic structures formed from continuous arrays of these particles have features as small as 50 nm. The quasi-continuous metallic structures formed in this fashion exhibit good effective conductivity, along with plasmon resonance absorption at a wavelength consistent with the plasmonic behavior of the constituent gold nanoparticles. The method presented here is well suited for the fabrication of micro- and nanoscale features

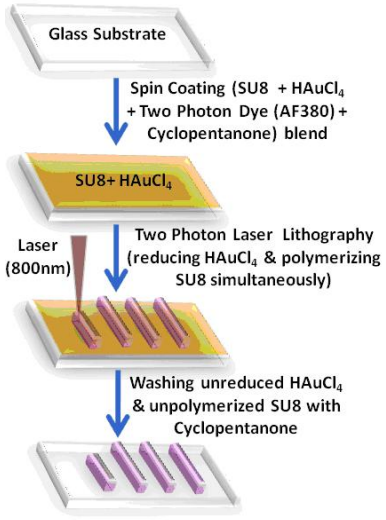

Figure . 2 TPL writing process steps (adapted from [6]).

because it is based on the initiation of a photochemical process in a small (sub-wavelength) focal volume. We discuss the writing method and present characterization of various functional structures along with simulations of their electromagnetic performance.

2 MATERIALS AND METHODS

The materials used for the writing process consisted of a negative phototoresist, SU-8 (Microchem Inc), that contains a small amount of photoacid generator; a two photon dye, AF380 (provided by US Air Force Research Laboratory, OH), which has a large two-photon absorption cross-section at 800 nm; and a gold precursor ($HAuCl_4.3H2O$ Sigma-Aldrich). These were dissolved in cyclopentanone, which is a good solvent for both SU-8 and $AuCl_4$. Films were produced on a glass cover-slip by spin-coating and typically have 1% AF380, 10% $HAuCl_4.3H2O$, and 89% SU-8 by mass, after solvent evaporation (Fig. 2). The writing was performed using a mode-locked femtosecond laser (Ti:sapphire laser with an operating wavelength of 800 nm, a pulse width of < 120 fs, and a repetition rate of 76 MHz). The dye absorbs energy at this wavelength and transfers energy to the photoacid generator, which decomposes producing a strong acid. This triggers both the gold ion reduction and the cationic polymerization of the photoresist. A writing speed of 50 μm per second was typically used for writing the structures in the film. The unexposed part was removed by dipping the film in cyclopentanone, then allowing it to air dry.

Typical metallic structures with a polymeric backbone are shown in Fig. 3. The SEM images illustrate the topography of the gold/polymer composite line, while the backscattered SEM in the inset more clearly demonstrates the presence of gold nanoparticles on the polymeric backbone, based on the large atomic-number-based contrast difference between gold and the polymer. Lines thus formed were a few hundred nanometers in width. By changing the laser power, we were able to tune the linewidth of the plasmonic feature from 1 μm to as small as 150 nm.

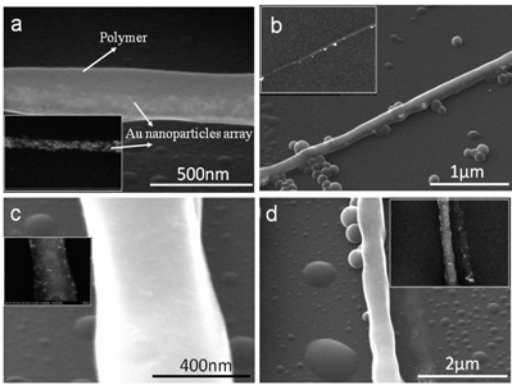

Figure 3: Secondary electron SEM images of polymeric nanostructures with embedded gold nanoparticles, written at (a) Low power; (b) Low power, imaged at lower magnification;(c) High power; (d) High power, imaged at lower magnification; insets show backscattered electron images of the corresponding structures (adapted from [6]).

We studied the effects of laser power and total photon dose on feature size by varying scanning speed and laser power, as shown in Fig. 4. The minimum power required for producing a detectable polymeric feature, 10-15 mW, did not differ appreciably between SU-8 alone and with gold precursor added, but at higher power this difference was more significant. The apparent width of the structures written at low power was ~750 nm for the gold doped polymer sample and about 1000 nm for the undoped SU-8. In both cases, the observed feature width was independent of laser power up to some threshold value (~30mW for polymer alone and ~50mW with gold precursor). Above that value, the line-width increased with increasing laser power, as shown in the inset of Fig. 4. We attribute the decrease in line-width and increase in the threshold for growth of line-width to coupling between the photoinitiation of cationic polymerization and the gold reduction. Essentially, it appears that these two processes compete for products of photoacid decomposition.

We developed a first-order analytical model to understand and predict the line width w for the writing process. We assume that the SU8 is polymerized at positions where the total photoacid generated exceeds a threshold value. The formula for the line width is

$$w = r_0 \left[\ln\left(\frac{\sqrt{\pi}\sigma_{2,eff} \nu \tau_L r_0 N_0^2}{2 \mathrm{v}_b C} \right) \right]^{1/2}, \qquad (1)$$

where N, defined by the wavelength λ of the incident light, the pulse repetition rate ν, the duration of the laser pulse τ_L during each repetition, and an average power P and $\sigma_{2,eff}$ is the "effective" two-photon cross section. We applied Eq. (1) to our experimental results and modeled w as a function of laser power P for the two photon-induced

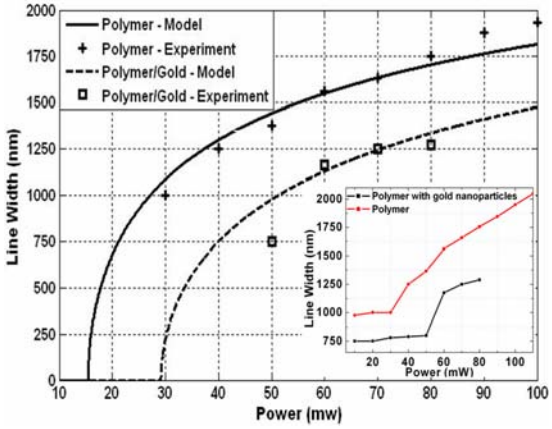

Figure 4: Polymerization line width vs. laser power: comparison of model with experimental data, inset shows the complete experimental data (adapted from [6]).

polymerization process, with and without the presence of the gold precursor. The theoretical and experimental results were in reasonable agreement as shown in Figure 4.

We characterized the electrical conductivity of the written lines. This is important because the level of conductivity of the fabricated structures will determine the range of utility of the writing process, especially as it pertains to applications requiring functional electronic materials. We used a four-point probe to measure conductivity of individual lines, as illustrated in Figure 5a,b. Figure 5c shows the current versus applied voltage for a structure that was prepared with 30 wt % gold precursor loading. The fabricated gold lines were 800 nm wide and 300 μm long, and their conductivity ranged from 1 to 2.5 x 10^7 mho/m, which is approximately 1/4 that of bulk gold. The relatively high conductivity of these structures is due to the high loading fraction of gold precursor and the photoreduction of the precursor into relatively small, densely packed gold nanoparticles.

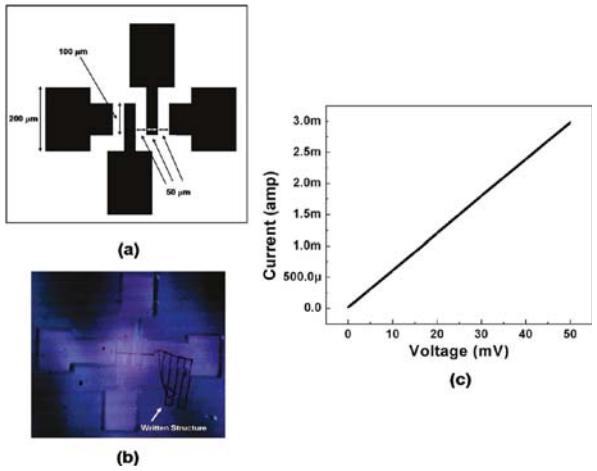

Figure 5. Electrical characterization of gold nanoparticle-doped line structure: (a) geometry of four-point probe measurement system; (b) four-point probe system; (c) current vs. applied voltage (adapted from [7]).

3 RESULTS AND DISCUSSION

We applied the method describe above to write various functional structures. Figure 6 shows examples of different ordered patterns of written structures, which demonstrates the versatility of the writing process. Figure 6a shows an electron micrograph of a gold "nanocauliflower" array. The diameter of a gold cauliflower element is 1 μm, and the periodicity is 2 μm. These structures were prepared using a high gold precursor loading (>30 wt %). Metal nanoblocks made at comparatively higher power are shown in Figure 6b. The length to width ratio of these structures is 2.5 μm/1.5 μm, and the distance between two elements is approximately 4 μm. Hexagonal ring structures have also been prepared, as shown in Figure 6c. Figure 6d shows a

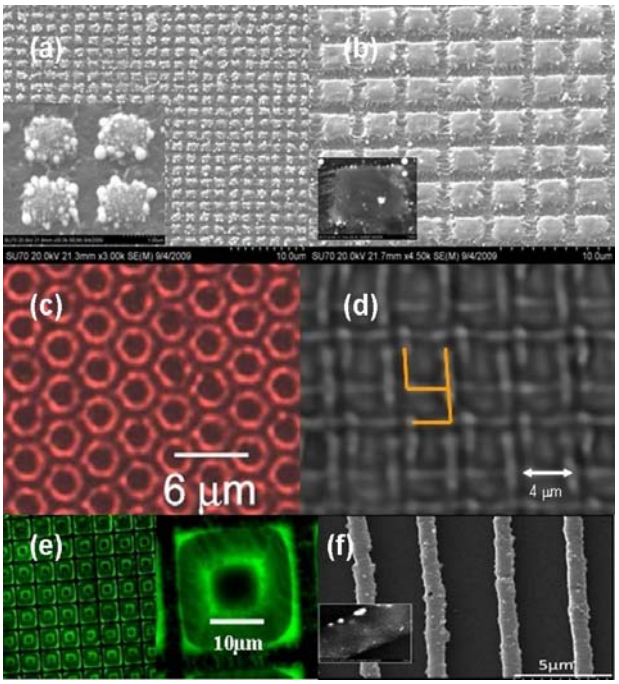

Figure 6: SEM images (a) nanocauliflowers and (b) nanoblocks; (insets in a and b show the close up view of elements); Confocal microscope image of (c) hexagonal ring structures; (d) chiral Y structures with highlighted geometry; (e) plasmonic donuts; and SEM image of (f) grating structure (adapted from [7]).

2D array of chiral Y structures, which calculations show can rotate the polarization of incoming light as described below. Figures 6e and 6f are images of plasmonic donut structures and a grating structure, respectively.

We performed simulations to understand the

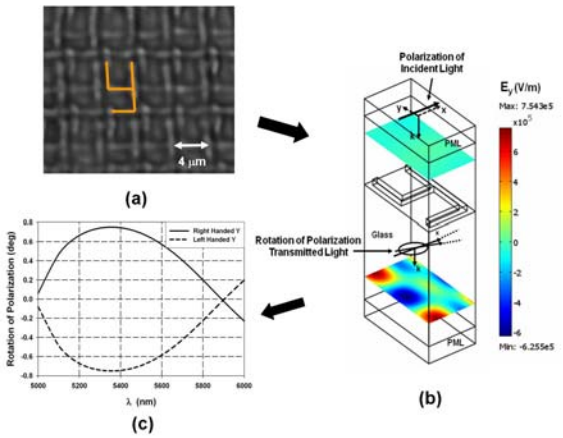

Figure 7. Electromagnetic analysis: (a) confocal transmission image of chiral Y structures; (b) computational model for a single structure showing the presence of an E_y component in the transmitted field, (c) plot showing rotation of polarization vs. λ in the transmitted field for right and left=handed structures.

electromagnetic (EM) response of the fabricated materials. The Comsol RF solver (www.Comsol.com) was used for time-harmonic field analysis of the transmission, scattering and absorption spectra of various structures. Figure 7 shows the computational model and predictions for a periodic array of chiral Y structures in which each Y structure is 8 μm in height, 4 μm wide and 600 nm deep. Neighboring elements are spaced 5 μm center-to-center in the width direction. Perfectly matched layers (PMLs) are applied at the top and bottom of the computational domain to reduce backscatter from these boundaries. The incident field is generated by a time-harmonic surface current source (not shown) positioned in the x-y plane immediately below an upper PML as discussed in [8-9]. The incident field is linearly polarized along the x-axis and the field propagates downward. The polarization of the transmitted field is rotated due to the chirality of the elements. We impose periodic boundary conditions about this element to account for the presence of its neighbors. We illuminate the element at normal incidence over a range of wavelengths, 5000-6000 nm, and we used a constitutive relation for the complex-valued permittivity of gold that is appropriate for these wavelengths. Note from Fig, 6c that the polarization is rotated in an opposite sense for right and left-handed orientations of Y, which is consistent with other published experimental and theoretical studies.

We performed similar EM analysis for various other fabricated structures. Figure 8 illustrates such an analysis of the nanoplasmonic cauliflower structure shown in Fig. 6a.

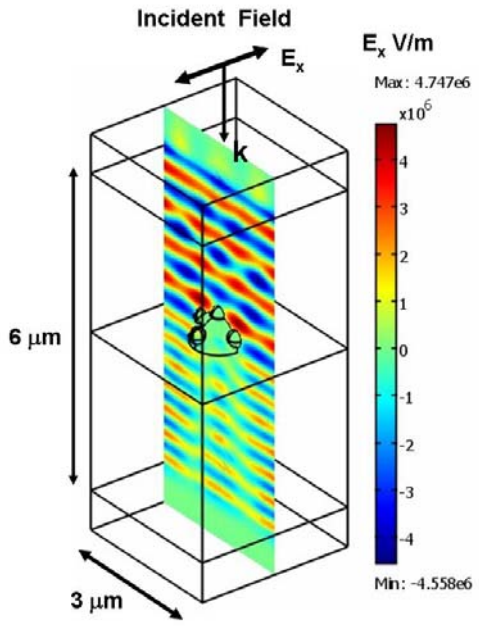

Figure 8. Electromagnetic analysis of the nanocauliflower structure showing E_x field component.

The illumination of this structure is as described above, i.e. the incident field is linearly polarized along the x-axis. This structure absorbed power at optical frequencies because of the complex-valued permittivity of the gold constituent. However, it does not exhibit a pronounced plasmon resonance because the 1 μm structure it greater than subwavelength.

4 CONCLUSIONS

We have demonstrated use of TPL to produce sub-wavelength metal nanoparticle-doped polymeric structures with line widths as small as 150 nm. The conductivity of the written lines is within a factor of 4 of that of bulk gold. We expect this novel approach of *in situ* fabrication of plasmonic structures on a polymeric backbone will allow efficient fabrication of new three-dimensional optically active structures with subwavelength feature sizes.

REFERENCES

[1] K. S. Lee, R. H. Kim, D. Y. Yang, S. H. Park, Advances in 3D nano/microfabrication using two-photon initiated polymerization, Progress in Polymer Science **33**, 631, 2008.

[2] C. N. LaFratta, J. T. Fourkas, T. Baldacchini, R. A. Farrer, Multiphoton fabrication, Angewandte Chemie International Edition. **46**, 6238, 2007.

[3] R. R. Gattass, E. Mazur, Femtosecond laser micromachining in transparent materials, Nature Photonics **2**, 219 2008.

[4] T. Nakahama, S. Yokoyama, H. Miki, S. Mashiko, Control of multiphoton process within diffraction limit space in polymer microstructures, Thin Solid Films **499**, 406, 2006.

[5] M. S. Rill, C. Plet, M. Thiel, I. Staude, G. von Freymann, S. Linden, M. Wegener, Photonic metamaterials by direct laser writing and silver chemical vapour deposition. Nat. Mater. **7**, 543-546, 2008.

[6] S. Shukla, E. P. Furlani, X. Vidal, M. T. Swihart and P. N. Prasad, Two-photon lithography of sub-wavelength metallic structures in a polymer matrix, Adv. Mater. **22**, 3695–3699, 2010.

[7] S. Shukla, X. Vidal, E. P. Furlani, M. T. Swihart, Kyoung-Tae Kim, Yong-Kyu Yoon, Augustine Urbas, and P. N. Prasad, Subwavelength direct laser patterning of conductive gold nanostructures by simultaneous photopolymerization and photoreduction, ACS Nano. **5** 3, 1947–1957, 2011.

[8] E. P. Furlani and A. Baev, "Optical nanotrapping using cloaking metamaterial," Phys. Rev. E, **79**, 026607, 2009.

[9] E. P. Furlani and A. Baev, "Free-space excitation of resonant cavities formed from cloaking metamaterial," J. Mod. Opt. **56**, 4 523-529, 2009.